CIRCULAR MICROCHANNELS ENHANCE DIODICITY PERFORMANCE AT ULTRA-LOW REYNOLDS NUMBER FOR MICROFLUIDIC BEAD-BASED DIODES

Ryan D. Sochol*, Jonathan Lei, Albert Lu, Erica L. Hicks, Shan Gao, Vivek Menon, Kosuke Iwai, Luke P. Lee and Liwei Lin

Berkeley Sensor and Actuator Center, University of California, Berkeley, USA

ABSTRACT

Self-regulating fluidic components are critical to the advancement of micro/nanofluidic circuitry for chemical and biological applications, including sample preparation on chip and point-of-care (POC) molecular diagnostics. Previously, a variety of diodic components have been developed to enable flow rectification in fluidic technologies (*e.g.*, microscale drug delivery systems in which backflow could be medically harmful). In particular, prior works have utilized suspended microbeads as dynamic resistive elements to achieve microfluidic diodes for ultra-low *Reynolds Number* (*i.e*., $Re < 0.25$) applications; however, using spherical beads to block fluid flow through rectangular channels is inherently limited. To overcome this issue, here we present a microfluidic bead-based diode that uses a targeted circular-shaped microchannel for microbead docking to rectify fluid flow under $Re \leq 0.25$ conditions. Experimental results revealed *Diodicities* (*Di*'s) ranging from 1.34±0.15 to 5.32±0.64 for *Re* varying from 0.05 to 0.25.

KEYWORDS

Diode, Check Valve, Microbead, Circular Microchannels

INTRODUCTION

Microfluidic components that facilitate automated "on-chip" functionalities, such as device-embedded flow switching and flow rectification, are in critical demand [1-3]. At the ultra-low *Re* flows associated with lab-on-a-chip technologies, the contribution of the non-linear inertial term of the *Navier-Stokes equation* is minimal, which renders "fixed-geometry" valves (*e.g.*, diffusers and Tesla valves) ineffective [3, 4]. To bypass this issue, researchers have developed double-layer "flap" valves capable of *Di*'s ranging from 1.1 to 4.6 (*i.e*., for $Re \approx 1$ to 35); however, prior reports have found that such valves fail at $Re <$ ~0.3 [4, 5]. Additionally, flap valves are manufactured *via* multi-layer microfabrication processes, which suffer from increased costs, time, and labor compared to single-layer lithographic processes. To overcome these limitations, Ou *et al.* presented a single-layer bead-based diode that utilized up to 850 suspended microbeads to rectify fluid flow at $Re < 1$ [6, 7]. Previously, we introduced a microfluidic bead-based diode that used only a single suspended microbead to achieve *Di*'s ranging from 1.14±0.01 to 2.51±0.03 for *Re* varying from 0.05 to 0.25 [8]. The major impediment toward achieving higher *Di*'s for prior bead-based diodes is that using *spherical* microparticles to block fluid flow through *rectangular* microchannels is inherently flawed. Thus, here we present a microfluidic bead-based diode that includes a *circular*-shaped microchannel for microbead docking (Fig. 1).

CONCEPT

Figure 1 shows illustrations of the diode concept, which operates similar to a ball check valve. Although the majority of the device consists of rectangular microchannels (18 μm in height), the diode chamber includes a circular docking channel for microbead trapping or releasing (*i.e.*, based on the flow polarity). Consistent with our prior single-microbead-based diode [8], here we employ our micropost array railing (μPAR) technique [9, 10] as a one-way 'track' to ensure that after a suspended polystyrene microbead (16.6 μm in diameter) enters the diode chamber, the bead is maintained within the chamber (*i.e.*, regardless of the flow polarity) because the microposts (15×15 μm^2) act as a physical barrier. For the forward flow case, the microbead releases from the diode docking position to facilitate fluid flow through the docking channel (Fig. 1a). For cases in which the flow polarity is reversed, the microbead re-immobilizes at the entrance of the docking channel, which obstructs fluid flow through the diode (Fig. 1b). This process can be repeated continuously by switching the flow polarity as desired.

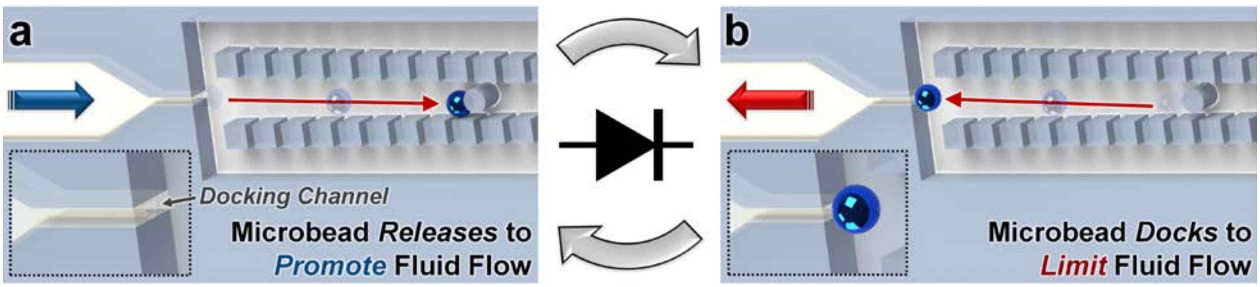

Figure 1. Conceptual illustrations of the microfluidic bead-based diode with a circular-shaped docking channel. (a) During forward flow, the microbead releases from the docking position to enable fluid flow through the channel. The bead remains within the diode chamber. (b) During reverse flow, the microbead immobilizes in the docking site, thereby obstructing fluid flow through the channel. This process functions autonomously based on the flow polarity.

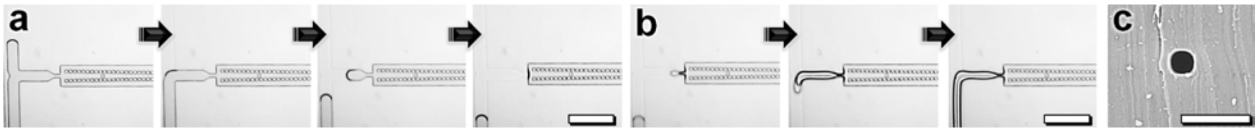

Figure 2. Experimental results for selectively fabricating a circular-shaped docking channel. (a) Initially, a separate inlet is used to load uncured PDMS into the docking channel. (b) After the PDMS has reached the base of the docking channel, pressurized air is used to displace the PDMS, leaving behind a circular cross-section. (c) SEM image of the cross-section of a fabricated circular docking channel. Scale Bars = (a, b) 200 µm, (c) 50 µm.

DEVICE FABRICATION

The microfluidic diode was constructed *via* standard photolithography and soft lithography methods as described previously [8-10]; however, to fabricate a targeted circular-shaped docking channel, we adapted a technique originally developed by Abdelgawad *et al.* [11]. Specifically, a separate inlet was initially used to vacuum-load uncured PDMS into the docking channel (Fig. 2a). Once the uncured PDMS filled the docking channel completely, pressurized air was inputted into the device to displace most of the PDMS, while leaving behind a circular-shaped cross-section (Fig. 2b). While continuing to input the pressurized air, the device was placed on a hot plate (set at 150 °C) for approximately 30 minutes to cure the PDMS (which consequently sealed the PDMS inlet as well). Figure 2c shows an SEM micrograph of the cross-section of a fabricated circular-shaped docking channel.

RESULTS

Sequential micrographs of microbead dynamics within the microfluidic bead-based diode are shown in Figure 3. During device operation, a single microbead was pre-loaded into the diode chamber *via* a separate inlet, which was sealed after the pre-loading process. As shown in Fig. 3a, our μPAR technique successfully guided the microbead from the initial flow stream into the diode chamber during reverse flow. After reversing the flow polarity (*i.e.*, to achieve forward flow), the microbead was released from the diode docking position, but remained within the diode chamber due to the arrayed microposts (Fig. 3b). To prevent the released microbead from becoming permanently lodged between adjacent sets of micropost array rails (separation angle = 2°), a circular micropost was included in the middle of the rails. By reversing the flow polarity again (*i.e.*, to achieve reverse flow), the microbead was transported to the entrance of the circular-shaped docking channel and subsequently immobilized (Fig. 3c). Experimental device runs with multiple external switches of the flow polarity revealed this process to be repeatable.

Quantified *Di* results for *Re* ranging from 0.05 to 0.25 are presented in Figure 4. For comparison purposes, experiments were also performed using *negative control* microdevices that did not include any loaded microbeads. The average *Di*'s for *Re* = 0.05 and 0.10 were 1.34±0.15 and 1.76±0.23, respectively, which were both statistically discernible from the negative control ($p < 0.05$). For comparatively larger *Re* of 0.15 to 0.25, experimental results revealed average *Di*'s ranging from 3.58±0.33 to 5.32±0.64, which were significantly higher than the negative control ($p < 0.0001$). Although these results mark an improvement in *Di* ranging from 17.5% to 112% *versus* prior single-microbead-based diodes that included rectangular channels [8], several factors may have limited the overall device performance. An ideal bead-based diode would include microbeads and docking channels that are perfectly spherical and circular, respectively; however, this was not the case for the current study. This issue may have also contributed to the observed enhancement of *Di* at relatively higher *Re*. For example, larger shear stresses impacting a docked microbead could potentially better lodge the bead by causing the elastomeric PDMS of the docking channel to deform (and better fit the shape of the microbead), which would increase the corresponding fluidic resistance.

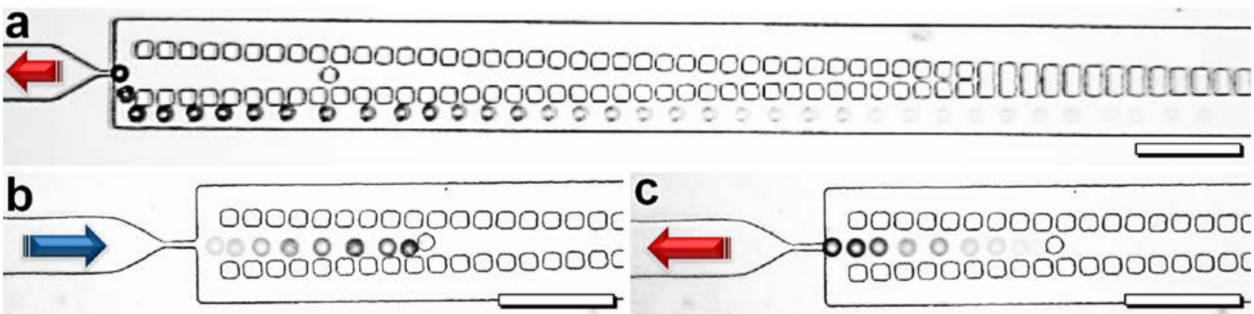

Figure 3. Overlaid sequential micrographs showing microbead dynamics in the microfluidic bead-based diode. (a) Initially, a single polystyrene microbead (ø = 16.6 µm) is pre-loaded into the diode chamber under reverse flow. Our micropost array railing (µPAR) technique [9, 10] *prevents the microbead from immobilizing until it reaches the entrance of the docking channel. (b) During forward flow, the microbead releases from the docking channel, but remains within the diode chamber due to the micropost array rails. The circular-shaped micropost (located between the micropost array rails) prevents the microbead from being wedged between the square-shaped microposts (separation angle = 2°). (c) During reverse flow, the microbead re-immobilizes at the entrance of the docking channel. Experimental observations revealed this process to be repeatable. Scale Bars = 100 µm.*

CONCLUSIONS

Emerging micro/nanofluidic technologies demand robust fluidic components that are capable of functioning autonomously under ultra-low *Re* conditions. Here, we presented a microfluidic bead-based diode that utilized a targeted circular-shaped channel for microbead docking. Experimental runs revealed *Di*'s within the range of 1.34±0.15 to 5.32±0.64, corresponding to *Re* varying from 0.05 to 0.25. These results mark an improvement over similar techniques that employ rectangular channels for docking spherical microparticles. Several adaptations of the presented technique could yield enhanced *Di*'s. For example, architectures in which numerous bead-based diodes are arrayed in series or in parallel could greatly improve the diodic performance. To develop ideal micro/nanofluidic particulate-based diodes, future work should focus on closely matching the shapes of suspended particles with the corresponding geometries of the docking channels.

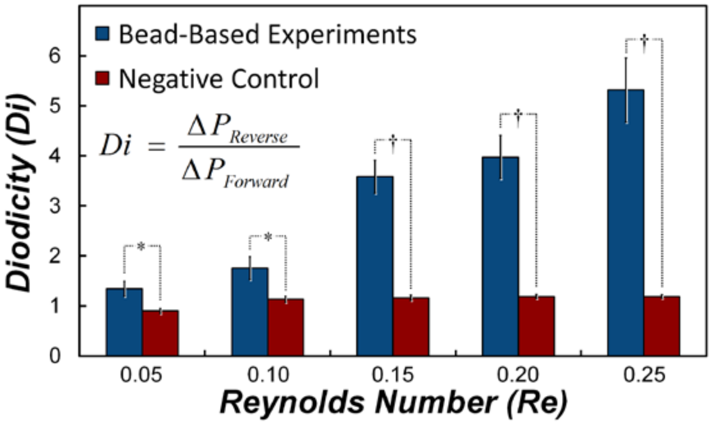

Figure 4. Experimental results for average Diodicity (Di) performance versus varying Reynolds Number (Re). $\Delta P_{Forward}$ *and* $\Delta P_{Reverse}$ *denote the pressure drop across the diode for the forward flow case (unobstructed docking channel) and the reverse flow case (obstructed docking channel), respectively. 'Blue' and 'red' bars correspond to experiments with or without a microbead, respectively; Error Bars denote s.e.m.; '*' and '†' denote* $p < 0.05$ *and* $p < 0.0001$ *statistically significant differences, respectively.*

ACKNOWLEDGEMENTS

The authors greatly appreciate the help and support of Thomas Brubaker, Deepak Lingam, Casey Glick, Nazly Pirmoradi, William Krieger, Adrienne Higa, and Paul Lum, as well as the members of the Liwei Lin Laboratory, the Biologically-inspired Photonics-Optofluidics-Electronics Technology and Science (BioPOETS) Laboratory, and the Micro Mechanical Methods for Biology (M^3B) Laboratory. This research is supported in part by the DARPA N/MEMS program under the Micro/Nano Fluidics Fundamentals Focus (MF3) center.

REFERENCES

[1] B. Mosadegh, C.-H. Kuo, Y.-C. Tung, Y.-S. Torisawa, T. Bersano-Begey, H. Tavana, and S. Takayama, *Integrated elastomeric components for autonomous regulation of sequential and oscillatory flow switching in microfluidic devices*, Nature Physics, pp. 433-437, (2010).

[2] B. Mosadegh, T. Bersano-Begey, J. Y. Park, M. A. Burns, and S. Takayama, *Next-generation integrated microfluidic circuits*, Lab on a Chip, pp. 2813-2818, (2011).

[3] A. Groisman and S. R. Quake, *A microfluidic rectifier: Anisotropic flow resistance at low Reynolds Numbers*, Physical Review Letters, pp. 094501, (2004).

[4] J. Loverich, I. Kanno, and H. Kotera, *Single-step replicable microfluidic check valve for rectifying and sensing low Reynolds number flow*, Microfluidics and Nanofluidics, pp. 427-435, (2007).

[5] M. L. Adams, M. L. Johnston, A. Scherer, and S. R. Quake, *Polydimethylsiloxane based microfluidic diode*, Journal of Micromechanics and Microengineering, pp. 1517-1521, (2005).

[6] K. Ou and M. Chiao, *A passive check valve using microspheres for low pressure and low flow rate applications*, Proc. of the 16th International Solid-State Sensors, Actuators and Microsystems Conference (Transducers 2011), pp. 1785-1788, (2011).

[7] K. Ou, J. Jackson, H. Burt, and M. Chiao, *Microspheres as resistive elements in a check valve for low pressure and low flow rate conditions*, Lab on a Chip, (2012). (DOI: 10.1039/C2LC40652G)

[8] R. D. Sochol, K. Iwai, J. Lei, D. Lingam, L. P. Lee, and L. Lin, *A single-microbead-based microfluidic diode for ultra-low Reynolds Number applications*, Proc. of the IEEE 25th International Conference on Micro Electro Mechanical Systems (MEMS 2012), Paris, France, pp. 304-307, (2012).

[9] R. D. Sochol, R. Ruelos, V. Chang, M. E. Dueck, L. P. Lee, and L. Lin, *Continuous flow layer-by-layer microbead functionalization via a micropost array railing system*, Proc. of the 16th International Solid-State Sensors, Actuators and Microsystems Conference (Transducers 2011), pp. 1761-1764, (2011).

[10] R. D. Sochol, S. Li, L. P. Lee, and L. Lin, *Continuous flow multi-stage microfluidic reactors via hydrodynamic microparticle railing*, Lab on a Chip, (2012). (DOI: 10.1039/C2LC40610A)

[11] M. Abdelgawad, C. Wu, W.-Y. Chien, W. R. Geddie, M. A. S. Jewett, and Y. Sun, *A fast and simple method to fabricate circular microchannels in polydimethylsiloxane (PDMS)*, Lab on a Chip, pp. 545-551, (2011).

CONTACT

*Ryan D. Sochol, tel: +1-410-935-8971; rsochol@gmail.com